

The Effects of Storm Events on Sediment, Nutrient, and Biofilm Dynamics in a Stream Recovering from Acid Mine Drainage

Natalie Kruse Daniels¹, Jennie Brancho¹, Morgan L. Vis²

¹*Environmental Studies Program, Voinovich School of Leadership and Public Affairs, Ohio University, Athens, Ohio 45701, USA, krusen@ohio.edu, ORCID 0000-0002-8684-1315*

²*Environmental and Plant Biology Department, Ohio University, Athens, Ohio 45701, USA, vis-chia@ohio.edu*

Abstract

This study quantified changes in nutrients, sediment transport, and algal biomass during normal and storm conditions in a treated acid mine drainage stream. Nitrate, sulfate, total reactive phosphorous (TRP), sediment deposition and total suspended solids (TSS) were measured during each sampling event. Biological response was measured by comparing algal biofilm biomass. Antecedent precipitation index (API) was an indicator of runoff potential. As API increased TSS increased, while chlorophyll a, conductivity, and sulfate decreased. TSS, nitrate, and sediment deposition were higher overall during storm events. TRP remained low at all sites during the sample period, suggesting phosphorous limitation.

Keywords: Phosphorus Limitation, Climate Change, Algae Biomass, Sediment Deposition, Antecedent Precipitation Index

Introduction

Although the effects of climate change on acid mine drainage (AMD) streams is an emerging area of research, several studies have investigated the effects of warming temperatures and changing precipitation regimes on metal toxicity, pyrite oxidation, and seasonal fluctuations in AMD generation and composition (Anawar 2013, Nordstrom 2009). Depending on the site and duration of the storm, AMD discharges from mines display one of three behaviors that affect acidity and contaminant concentrations in the stream. During high flow, reaction sites may be cut off from oxygen required to form AMD due to flooding. This phenomenon is known as sparing (Kruse *et al.* 2014). Sparing causes contaminant concentrations to increase at a slower rate than discharge due to dilution and slower rates of AMD formation (Kruse *et al.* 2014, Mack *et al.* 2014). Alternatively, AMD discharges may exhibit flushing behavior. Flushing occurs when contaminant concentrations increase at a faster rate than discharge (Kruse *et al.* 2014), and this phenomenon may occur for several different reasons. Following heavy precipitation or

snowmelt, water can overflow the most accessible mine pools and spill over into disconnected pools that are only accessible during high flow events. This increased connection to mine pools results in greater generation of AMD and higher contaminant loads (Mack *et al.* 2014). Flushing may also be caused by the faster dissolution of soluble salts during heavy storms (Nordstrom 2009). If neither flushing nor sparing occurs, AMD contaminant concentrations will increase at the same rate as discharge (Kruse *et al.* 2014). Systems may display different behaviors relative to the duration of the storm, with flushing more likely to occur at the beginning and sparing later during prolonged storms (Kruse *et al.* 2014, Nordstrom 2009). The rates of AMD generation during storms are likely to be site-specific (Kruse *et al.* 2014). AMD contaminant concentrations following storm events are hysteretic, depending on the duration and frequency of storm events (Nordstrom 2009).

Storm events can also impact contaminant concentrations by scouring sediments from the streambed. In AMD systems, the majority of these sediments are metal hydroxides. By

scouring sediments, storms uncover new sediments onto which heavy metals and nutrients can sorb (Chapman *et al.* 1983). Depending on the behavior of AMD generation during storm events, such scouring can reduce heavy metal and/or nutrient loads or prevent drastic spikes in concentrations that may have toxic or otherwise harmful effects. However, scouring of sediments and subsequent generation of new metal hydroxides may further limit biofilms by smothering communities and decreasing light availability (Smucker and Vis 2011).

Increased storm frequencies and intensities may also alter nutrient retention and transport on a catchment level. Precipitation events restore connections between terrestrial landscapes and the aquatic ecosystems, allowing transport of pollutants from other land uses within the watershed into the stream via runoff. Once in the stream, nutrients are either stored in biomass, soil, or groundwater, transported back to the atmosphere as a gas (e.g. nitrogen), or carried downstream (Welter and Fisher 2016). Nutrients typically associated with sediment include ammonium, particulate organic nitrogen, and phosphorous (Lloyd *et al.* 2016). Substantial proportions of the annual sediment (Inamdar *et al.* 2017) and total phosphorous (Lloyd *et al.* 2016) export load have been attributed to the most intense storm events of that year. Storm events may contribute to higher nutrient concentrations via nitrogen and phosphorous loading from runoff or lower nutrient concentrations via greater export of sediments and nutrients.

Study Site

The fourth largest tributary to Raccoon Creek (Kruse *et al.* 2013), Hewett Fork is located within the headwaters of Raccoon Creek (Kruse *et al.* 2012). Hewett Fork is approximately 24.8 km long, and the subwatershed drains 104.9 km². The confluence of Hewett Fork and Raccoon Creek occurs at river kilometer (RKM) 144.2 on Raccoon Creek (Kruse *et al.* 2013). Sediment dynamics, nutrient concentrations, and biofilm abundance were measured at six sampling sites within Hewett Fork: HF137, HF095, HF090, HF060, HF045, and HF039.

HF137 is upstream of the Carbondale Doser and the confluence of Carbondale Creek and Trace Run with Hewett Fork. This site is not currently impacted by AMD. Therefore, HF137 was used as the reference site for this study. The remaining five sites were used as the experimental group. HF095 and HF090 are located within the impaired zone, HF060 and HF045 within the transition zone, and HF039 within the improved zone.

Field Methods

Sediment transport, nutrient concentrations, and biofilm communities were measured at all six sites during normal and storm conditions. Sampling began May 28, 2018 and ended November 1, 2018 to capture three important annual hydrologic events: heaviest storms in spring, lowest flow in summer, and poorest water quality in fall. Prior to each sampling event, a Myron Ultrameter II datasonde was calibrated. The pH probe was calibrated using standard solutions with pH values of 7, 4, and 10 in that order. The conductivity probe was calibrated using a standard solution of 1413 $\mu\text{S}/\text{cm}$. At each site, several field parameters were collected using the Myron Ultrameter II datasonde. Water temperature was immediately recorded in degrees Celsius. Then, the Myron Ultrameter II datasonde was set aside to allow the meter to settle before measuring pH and conductivity.

Nutrient Concentrations

Three nutrient concentrations were measured at each site during each sampling event: nitrate (NO_3^-), sulfate (SO_4^{2-}), and total reactive phosphorous. At each site, one 1 L water sample was collected in an HPDE bottle, filtered at the lab, and partitioned into subsamples for each measurement. Total reactive phosphorous subsamples were kept frozen at -20 °C until analysis. To prevent interference from iron in phosphate measurements, total reactive phosphorous samples were prepared using the ascorbic acid/colorimeter method (Stainton *et al.* 1976). Total reactive phosphorous concentrations were measured using a Genesys™ 20 Visible Spectrophotometer (Thermo Fisher Scientific Inc. Waltham, MA). Nitrate and sulfate concentrations were measured within

48 hours of sample collection using a HACH DR/890™ colorimeter (Hach Company, Loveland, CO) with HACH powder pillow reagents (Hach Company 2009). Nitrate concentrations were measured using the cadmium reduction method (method 8192) (Hach Company 2015), while sulfate concentrations were measured using the US EPA SulfaVer 4 Method (method 8051) (Hach Company 2018).

Sediment Deposition

Sediment traps were constructed and deployed in the streambed on April 30 at each site to measure deposition, consisting of 36 plastic containers (3 in. by 3 in. by 2 in.) nested in a plastic rack. A pre-weighed amount of dry river rock was placed into each sampling container prior to deployment to weigh the trap down. The sediment traps were dug into the bed to ensure the tops of each container were flush with the bed to maximize sediment capture. During each sampling event, three containers were removed at random from the sediment traps at each site as replicates. At the lab, sediment deposition samples were emptied into pre-weighed aluminum trays. These samples were then placed into the oven until dry and weighed. Grain size analysis was conducted every fourth sampling event. Once the sediment deposition samples were fully dried, they were passed through a series of two sieves, one with a mesh size of 2 mm and the other 425 µm. The amount of sediment in each sieve was weighed, and the total weight from both sieves was subtracted from the total deposition sample weight.

Sediment Transport

Sediment transport through the water column was quantified by measuring total suspended solids (TSS) according to method 2540 (American Public Health Association *et al.* 2005). Prior to sample collection, 22 filters (0.45 µm) were rinsed and dried for one hour. These filters were then placed in a desiccator until analysis. During each sampling event, a 1 L water sample was collected in an HDPE bottle at each site and placed on ice for transport back to the lab. These samples were placed in the refrigerator and analyzed within 48 hours of collection. The 1 L water sample

was shaken to homogenize and then divided into three 300 mL replicate subsamples per site. Each subsample was filtered onto the pre-weighed filter paper using a MultiVac 310-MS-T Vacuum Filtration System (New Star Environmental, Roswell, GA). For quality control, two blank samples were filtered per sampling event. These samples were placed into the laboratory oven and allowed to dry for 1 hour at 100 °C. After drying, the samples were put into the desiccator to cool to room temperature and the mass of sediment measured. The resulting TSS values for each subsample were averaged to generate one TSS value per site per sampling event.

Biofilm Abundance

At each site, ten cobbles were randomly selected to analyze the biofilm communities on the substrate. Using a soft brush, biofilm was scrubbed from a 25 cm² area on each rock into a single sample; this sample was placed in a labeled and preweighed 20 mL scintillation vial. These vials were kept on ice for transport to the laboratory and then kept frozen. At the lab, each sample was freeze-dried for a minimum of 48 hours. The scintillation vials were weighed again once dry. Chlorophyll a Analysis – Chlorophyll a concentrations were analyzed according to EPA method 445.0 (Arar and Collins 1997). The weight of each of the borosilicate tubes was recorded prior to and following the addition of 2-4 mg of sample. Three borosilicate tubes were used for each sample as replicates. To each tube, 10 mL of 90% acetone was added. Tubes were covered in plastic wrap and aluminum foil and placed in the freezer for 24 hours. After 24 hours, chlorophyll a concentrations were measured using a Turner TD-700 fluorometer (Turner Designs, Sunnyvale, CA). An amount of 0.1 M HCl was added to each sample to account for phaeophytin-a.

Results

Measured using total annual precipitation (cm), 2018 has been the wettest year on record since the Carbondale doser was installed in 2004. Antecedent Precipitation Index (API) values were calculated for each day in 2018 and correlated with other variables. In Figures 1 and 2, trends in normal and storm conditions.

Conductivity decreased as water quality improved with distance from the doser. The highest conductivity value was measured as 1100 $\mu\text{S}/\text{cm}$ at HF039 on July 19. All other values ranged from 198.1 $\mu\text{S}/\text{cm}$ to 673.0 $\mu\text{S}/\text{cm}$. Each site followed relatively the same pattern as the reference site, though downstream sites experienced less variation during fall sampling events (HF060, HF045, and HF039 in September and October). Conductivity was significantly negatively correlated with API ($p = 0.0003$, $r_2 = -0.8009$). In normal and storm conditions, the conductivity decreased as API increased. The correlation between pH and API was not significant ($p = 0.0735$, $r_2 = 0.4751$). The pH did not show any clear differences between normal and storm conditions when plotted against API. Like conductivity, sulfate concentrations decreased as water quality improved further downstream from the doser. Sulfate concentrations were highest between July and September. All sites showed the same pattern of changes in sulfate over the sample period. Median sulfate concentrations were significantly correlated with API ($p = 0.0000$, $r_2 = -0.8886$). In both normal and storm conditions, sulfate decreased as API increased.

Nitrate concentrations varied greatly at each site over the sample period. Nitrate concentrations were not significantly correlated with API ($p = 0.9607$, $r_2 = -0.0139$). No pattern was discerned between API and nitrate. Nitrate concentrations were overall higher in storm events than normal events, though storm concentrations also varied greatly. Total reactive phosphorous concentrations peaked during the first sampling event on May 28. However, all concentrations measured during the sample period were between 0 mg/L (below detection) and 0.0018 mg/L. Most concentrations measured after the initial sampling event were below detection. As a result, the correlation between phosphorous and API was not significant ($p = 0.5575$, $r_2 = -0.1647$), and no pattern between phosphorous and API or weather was detected.

Over the course of the sampling period, sediment deposition followed the same pattern as the reference site for all sites

except HF045. HF045 experienced much less deposition and resuspension than the rest of the sites. At all sites, the highest sediment deposition values occurred between June and mid-July and again at the end of October, while the greatest resuspension values also occurred in mid-July (July 19). No significant correlation was found between median sediment deposited per day and API ($p = 0.2653$, $r_2 = 0.3073$). Additionally, no clear pattern between sites or API values was observed. Sediment deposition was more likely to be higher during storm events, though high variation was found in both weather conditions. Compared to the reference site, TSS varied more in all sites, with sites further downstream deviating more from the pattern seen at HF137 than the upstream sites. TSS at HF095 and HF090 peaked during June, HF060 and HF045 peaked during July, and TSS at HF039 peaked in September. HF045 experienced the greatest variation in TSS values during the sample period. Median TSS was significantly positively correlated with API ($p = 0.0141$, $r_2 = 0.6380$). However, TSS values showed different patterns in normal and storm conditions. During normal conditions, TSS did not show a clear trend with API. TSS increased with increasing API during storm conditions.

At the reference site, chlorophyll a peaked during the final sampling event on October 22. At all other sites, however, chlorophyll a peaked during August. Chlorophyll a was consistently low at all sites during June and began to increase in mid-July. In September, chlorophyll a values decreased again at all sites, followed by another increase in October. The highest peaks in chlorophyll a were measured at HF045 and HF137, the reference site. Median chlorophyll a was significantly negatively correlated with API ($p = 0.0156$, $r_2 = -0.6107$). Chlorophyll a decreased as API increased in both normal and storm conditions. This trend was slightly clearer in storm than normal conditions.

Discussion

The hypotheses tested in this study are partially supported by the data. While downstream sediment transport increased during storm events, this increase did not coincide with a

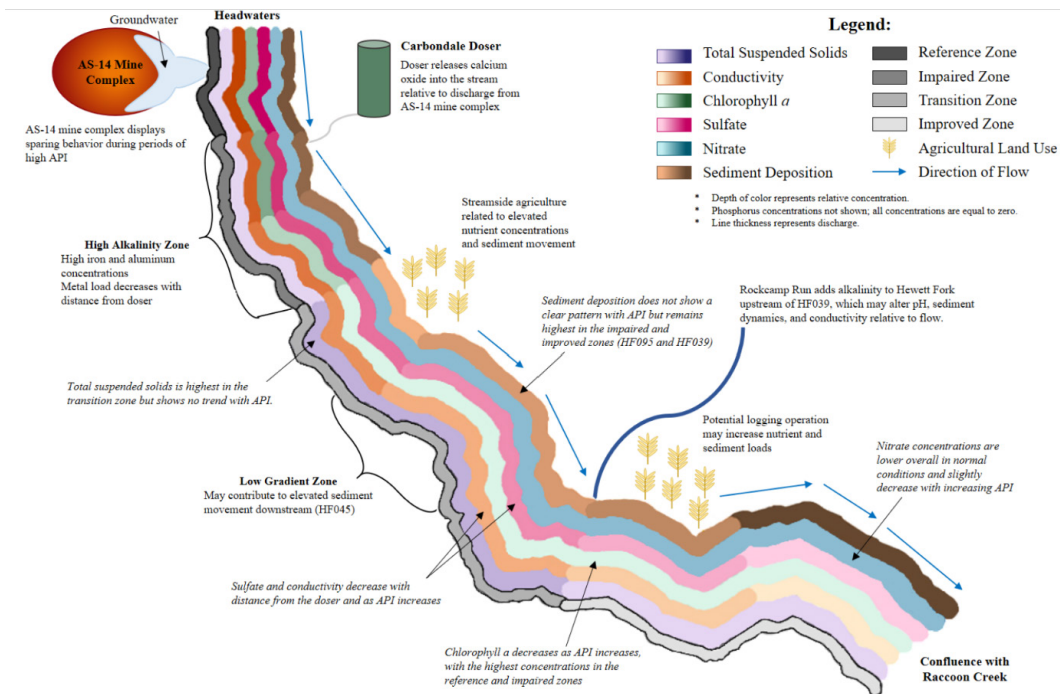


Figure 1 Conceptual model of sediment, nutrient, and biofilm dynamics in normal flow conditions.

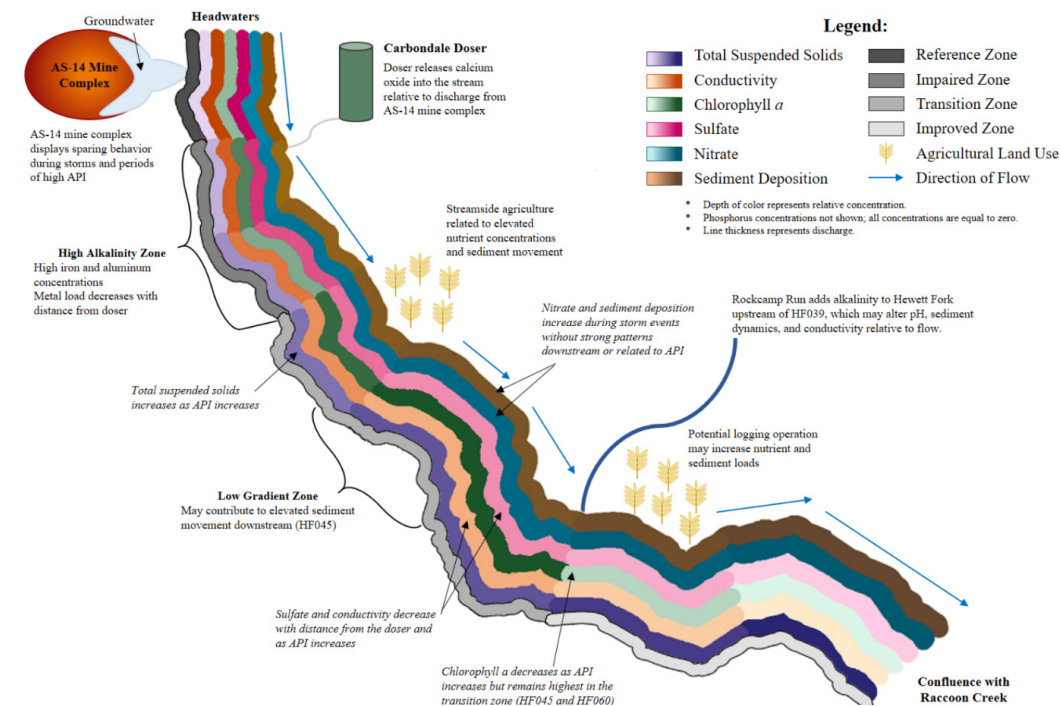


Figure 2 Conceptual model of sediment, nutrient, and biofilm dynamics in storm conditions.

decrease in nutrient concentrations. Instead, phosphorous concentrations remained low in all weather conditions, and nitrate showed only a slight increase during storms. The relationship between sediment transport and chlorophyll a was more complicated than hypothesized. High chlorophyll a values coincided with periods of low sediment deposition at most sites, but peaks in TSS values occurred at the same time as peaks in chlorophyll a at HF045 and HF039.

The parameters measured in this study may be affected by a variety of factors, including the Carbondale doser treatment system, AS-14 mine complex, and surrounding land use. During normal weather conditions, sulfate, conductivity, and chlorophyll a decreased with increases in API. Nitrate, TSS, and sediment deposition did not show any trend with API during normal weather conditions. TSS, nitrate concentrations, and sediment deposition showed high variation in normal weather conditions, but nitrate did show a slight increase in concentration as water quality improved downstream. Sediment deposition did not show a clear trend related to water quality with highest deposition rates in the impaired and improved zones. Sulfate and conductivity each decreased as water quality improved downstream. TSS, on the other hand, was highest in the transition zone. In storm conditions, TSS increased and sulfate, conductivity, and chlorophyll a decreased with increasing API. Sediment deposition and nitrate were each slightly higher in storm conditions, though both parameters showed high variability and no clear pattern related to API or water quality. Sulfate and conductivity decreased downstream as water quality improved. TSS increased downstream with the highest concentrations in the improved zone. Chlorophyll a was highest in the transition zone during storm events.

Conclusions

Climate change may affect AMD streams by altering geochemical processes and sediment and nutrient transport patterns. These changes may in turn have negative impacts on the biological communities living in the stream. Overall, API seemed to exert strong controls on stream characteristics, altering biofilm

communities and concentrations of both AMD pollutants and suspended sediments. Nutrient patterns were not as strongly linked to API, though nitrate concentrations were higher during storm events. This study also found very low concentrations of phosphorous. Like previous studies, these low concentrations indicate that AMD streams are likely phosphorous limited.

References

- Anawar HM (2013) Impact of climate change on acid mine drainage generation and contaminant transport in water ecosystems of semi-arid and arid mining areas. *Phys Chem Earth* 58-60: 13-21
- Arar E, Collins GB (1997) In vitro determination of chlorophyll a and phaeophytin a in marine and freshwater algae by fluorescence. 1st ed. USEPA. Office of Research and Development. Cincinnati, Ohio
- Chapman BM, Jones DR, Jung RF (1983) Processes controlling metal ion attenuation in acid mine drainage streams. *Geochimica et Cosmochimica Acta* 47: 1957-1973
- Hach Company. 2015. Nitrate cadmium reduction method 8192. Loveland, CO
- Hach Company. 2018. Sulfate US EPA SulfaVer 4 Method 8051. Loveland, CO
- Hach. 2009. DR/820, DR/850, DR/890 Portable datalogging colorimeter instrument manual. 2nd ed. Hach Company 68 pp
- Inamdar S, Johnson E, Rowland R, Warner D, Walter R, Merritts D (2017) Freeze-thaw processes and intense rainfall: the one-two punch for high sediment and nutrient loads from mid-Atlantic watersheds. *Biogeochem* 1-17
- Kruse NA, Bowman JR, Mackey AL, McCament B, Johnson KS (2012) The lasting impacts of offline periods in lime dosed streams: a case study in Raccoon Creek, Ohio. *Mine Water Environ* 31(4): 266-272
- Kruse NA, DeRose L, Korenowsky R, Bowman JR, Lopez D, Johnson KS, Rankin E (2013) The role of remediation, natural alkalinity sources, and physical stream parameters in stream recovery. *J Environ Manag* 128: 1000-1011
- Kruse NA, Stoertz MW, Green DH, Bowman JR, Lopez DL (2014) Acidity loading behavior in coal-mined watersheds. *Mine Water Environ* 33(2): 177-186

- Lloyd CEM, Freer JE, Johnes PJ, Collins AL (2016) Using hysteresis analysis of high-resolution water quality monitoring data, including uncertainty, to infer controls on nutrient and sediment transfer in catchments. *Sci Tot Environ* 543(A): 388-404
- Mack, B., J. Skousen, and L. M. McDonald. 2014. Effect of flow rate on acidity concentrations from above-drainage underground mines. *Mine Water Environ* 34(1): 50-58
- Nordstrom DK (2009) Acid rock drainage and climate change. *J Geochemical Exploration* 100: 97-104
- Smucker NJ, Vis ML (2011) Acid mine drainage affects the development and function of epilithic biofilms in streams. *J N Am Benthological Soc* 30(3): 728-738
- Stainton MP, Capel MJ, Armstrong FAJ (1977) *The Chemical Analysis of Freshwater*. 2nd ed. Fisheries and Environ Canada. Fisheries and Marine Service. Winnipeg, Manitoba, Canada
- Welter JR, Fisher SG (2016) The influence of storm characteristics on hydrological connectivity in intermittent channel networks: implications for nitrogen transport and denitrification. *Freshwater Bio* 61: 1214-1227